NANO LETTERS

Letter

pubs.acs.org/NanoLett

Mapping Intracellular Temperature Using Green Fluorescent Protein

Jon S. Donner,[†,∥] Sebastian A. Thompson,[†,∥] Mark P. Kreuzer,[†] Guillaume Baffou,[‡] and Romain Quidant*[,†,§]

[†]ICFO-Institut de Ciencies Fotoniques, Mediterranean Technology Park, 08860 Castelldefels (Barcelona), Spain

[‡]Institut Fresnel, Aix-Marseille Université, CNRS, Domaine Universitaire Saint Jérôme, 13197 Marseille Cedex 20, France

[§]ICREA – Institució Catalana de Recerca i Estudis Avançats, 08010 Barcelona, Spain

Supporting Information

ABSTRACT: Heat is of fundamental importance in many cellular processes such as cell metabolism, cell division and gene expression.[1−3] Accurate and noninvasive monitoring of temperature changes in individual cells could thus help clarify intricate cellular processes and develop new applications in biology and medicine. Here we report the use of green fluorescent proteins (GFP) as thermal nanoprobes suited for intracellular temperature mapping. Temperature probing is achieved by monitoring the fluorescence polarization anisotropy of GFP. The method is tested on GFP-transfected HeLa and U-87 MG cancer cell lines where we monitored the heat delivery by photothermal heating of gold nanorods surrounding the cells. A spatial resolution of 300 nm and a temperature accuracy of about 0.4 °C are achieved. Benefiting from its full compatibility with widely used GFP-transfected cells, this approach provides a noninvasive tool for fundamental and applied research in areas ranging from molecular biology to therapeutic and diagnostic studies.

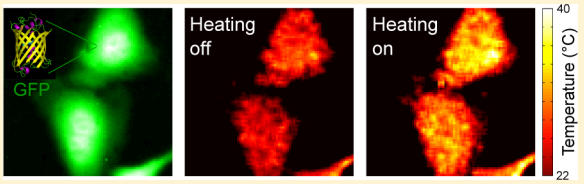

KEYWORDS: *Thermal imaging, GFP, cancer cells, fluorescence imaging, anisotropy*

Several microscopy techniques have recently been proposed to address the need for monitoring intracellular temperature in molecular biology. Most of them rely on introducing synthetic nano-objects into living cells such as quantum dots,[4,5] nanogels,[6] nanoparticles,[7] or thermosensitive dyes[8] whose fluorescence properties (intensity or spectrum) depend on temperature. In practice, however, such techniques suffer from some limitations. On the one hand, approaches based on fluorescence intensity measurements lack reliability since fluorescence intensity is dependent on many other factors such as molecular concentration, migration, bleaching, and illumination intensity. On the other hand, techniques based on spectral fluorescence measurements are usually slow (compared with intensity based techniques) as they require significant integration times. Incidentally, this second approach generally results in a single-point temperature measurement and not in real-time temperature imaging. Independently of these issues of reliability and slow read-out, introducing artificial probes within cells may alter their behavior or integrity.

Two alternative approaches have been reported very recently. The first is based on transfecting *E. coli* bacteria with a temperature sensitive vector that increases quantities of β-galactosidase in response to a temperature increment.[9] The heating of individual bacteria was monitored via an increase of the lacZ expression. However, such an approach is slow for real-time measurement and does not permit dynamic temperature monitoring because of its nonreversibility. The second approach uses a submicrometer thermocouple that is inserted into the cytoplasm of the cell.[10] This technique enables time-resolved measurement of changes in the cytoplasm temperature with high-temperature resolution. However, the introduction of a physical object through the plasma membrane may compromise the cells integrity and is incompatible with imaging.

The present work is motivated to address the limitations of the existing approaches to provide scientists with a temperature imaging technique that combines full biocompatibility with high resolution and fast read-out. We demonstrate how GFP can be used as an efficient temperature nanoprobe by measuring its fluorescence polarization anisotropy (FPA). GFP is already a widely used and important contrast agent in biology.[11] Several features explain the widespread use of GFP. (i) GFP can be expressed in many living organisms by genetic engineering making it a natural and noninvasive marker for in vivo applications;[11] (ii) over the last 15 years many GFP derivatives have been engineered so that they span the entire visible spectrum and have high quantum efficiency;[12] and (iii) GFP has been extensively researched and found useful for many applications as markers for gene expression, protein localization, and folding, as a Ca^{2+} ion or pH-sensor, redox-sensitive indicator, and as probes for protein−protein interactions.[13−16] Following this trend, we here propose to use GFP as a temperature sensor through FPA measurements.

The underlying physics relating temperature and molecular FPA is well established. In general, a population of fluorophores illuminated by a linearly polarized light re-emits partially

Received: January 30, 2012
Revised: March 6, 2012
Published: March 6, 2012

   dx.doi.org/10.1021/nl300389y | *Nano Lett.* 2012, 12, 2107−2111

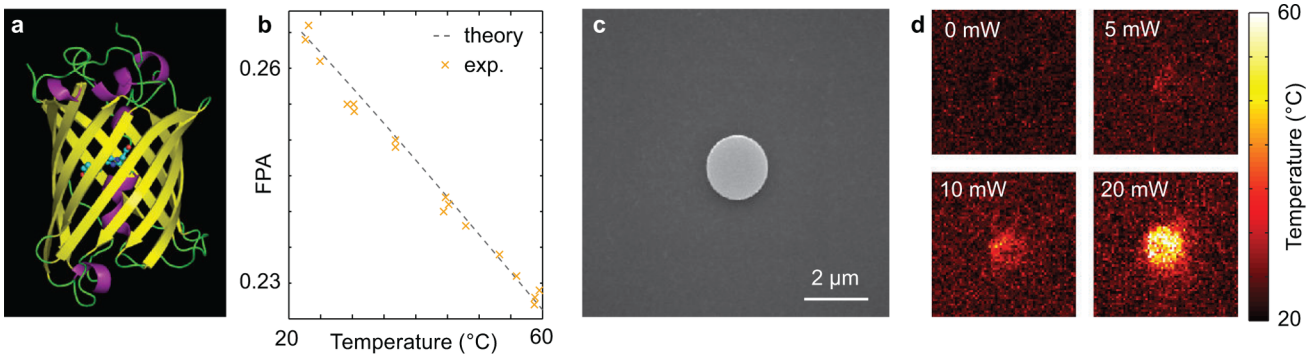

Figure 1. Measuring temperature around micro structures using GFP. (a) A 3D representation of the structure of GFP. (b) Calibration curve that relates between FPA of GFP and temperature in PBS. (c) Scanning electron microscope image of a lithographically imprinted gold microdisc. (d) Temperature map obtained around the microdisc while heating using an infrared laser.

polarized fluorescence due to the random orientation of the molecular dipoles.[17] The polarization anisotropy, r of the fluorescence is defined as

$$r = \frac{I_{\parallel} - I_{\perp}}{I_{\parallel} + 2I_{\perp}} \quad (1)$$

Where $I_{\parallel}$ and $I_{\perp}$ are the intensities of the fluorescence polarized parallel and perpendicular to the incident polarization. The measured value r is closely related to molecular rotation caused by Brownian dynamics according to Perrin's equation

$$\frac{1}{r} = \frac{1}{r_0}\left(1 + \frac{\tau_F}{\tau_R}\right) \quad (2)$$

where τ_R and τ_F are rotational and fluorescence life times, respectively, and r_0 is a constant named "limiting anisotropy" (usually close to 0.4). When the temperature increases, the Brownian rotational motion of the fluorophores is accelerated. Hence, the molecules will rotate more during their fluorescence lifetime. The more the molecules rotate during their fluorescence lifetime, the more the re-emitted photons will lose the memory of the incident light polarization. Consequently, a temperature increase leads to a decrease of the degree of polarization (anisotropy) of the fluorescence. Because FPA is a ratio of intensities, it is not sensitive to changes in absolute intensities that can be caused by photobleaching, variations of illumination intensity or fluorophore migration. Using a suitable calibration, FPA leads to an absolute temperature measurement. This is one of the main advantages of this technique.

Note that the maximum temperature sensitivity is reached when τ_R is on the order of τ_F. τ_R depends on the temperature T, the viscosity $\eta(T)$, and the hydrodynamic volume V of the fluorophore according to the Debye–Stokes–Einstein equation

$$\tau_R = \frac{V\eta(T)}{k_B T} \quad (3)$$

where k_B is the Boltzmann constant. Hence, V and η are the parameters one can play with to optimize the sensitivity of the technique (i.e., to ensure that τ_R is on the order of τ_F). For instance, for common fluorescent molecules (approximately 1 nm in size) in aqueous media ($\eta = 10^{-3}$ Pa · s at 25 °C), $\tau_R \sim 10^{-10}$ s which is 1 order of magnitude smaller than usual fluorescence lifetime ($\tau_F \sim 10^{-9}$ s). The rotational Brownian motion is too fast and the FPA is zero independently of the temperature. One way to solve this problem is to increase the viscosity η of the medium for instance by using a glycerol–water (4:1 wt) mixture.[18−20] However, such an approach is prohibitive for any application in biology for obvious reasons. In this work, we propose to increase the hydrodynamic volume V instead of the viscosity by using GFP. The characteristic size of GFP is 3.5 nm.[21] By coincidence, such a large protein leads to a rotational correlation time τ_R = 4.1 ns in water, which is on the order of magnitude of its fluorescence lifetime τ_F = 2.5 ns. The theoretical and experimental temperature dependence of the FPA of GFP in phosphate buffer saline solution (PBS), pH = 7.4, is presented in Figure 1b, for temperatures between 20 and 60 °C (∼ 76 °C being the denaturation temperature of GFP[22]). To estimate the temperature error of our measurement we took the standard deviation of the data giving 0.4 °C. Because of varying pH found in biological organisms, the experiment was reproduced at pH = 6.0 thus covering the typical range experienced within a cellular environment and the same results were obtained as shown in the Supporting Information section (Figure S1). The FPA variation over this temperature range is about 0.001/°C. The theoretical fit was performed from eqs 1 to 3, using fluorescence lifetime τ_F = 2.5 ns,[23] hydrodynamic volume V_{GFP} = 17.2 nm^3,[24] and limiting anisotropy r_0 = 0.31.

To begin we chose to illustrate GFP-based thermal imaging on a simple model system consisting of a gold microdisc (2 μm in diameter and 40 nm thick) prepared by standard e-beam lithography. The disk lies on a glass substrate and is surrounded by a PBS solution containing GFP molecules (3×10^{-5} M), all placed in the sample plane of a confocal optical microscope operated with two laser sources: a heating IR laser and a blue laser for GFP excitation (see Supporting Information). The spatial resolution of our method is limited by the diffraction limit of our collection path. In our case, we are exciting GFP with a 473 nm laser and collecting with an objective of NA = 1.0. Considering that the fluorescence of the GFP is below 600 nm, this leads to a diffraction limit smaller than 300 nm. To ensure that we obtain this resolution we performed the scan with a step size smaller than the diffraction limit, which is 100 nm in this case. An expected decrease of the FPA was observed around the structure while heating (i.e., during IR illumination). The associated temperature map obtained using the calibration curve of Figure 1b is presented in Figure 1d. The temperature increase is proportional to the power of the heating IR laser as expected.

We now present temperature measurements on single living cells. We chose to work with transfected HeLa and U-87 MG

dx.doi.org/10.1021/nl300389y | Nano Lett. 2012, 12, 2107−2111

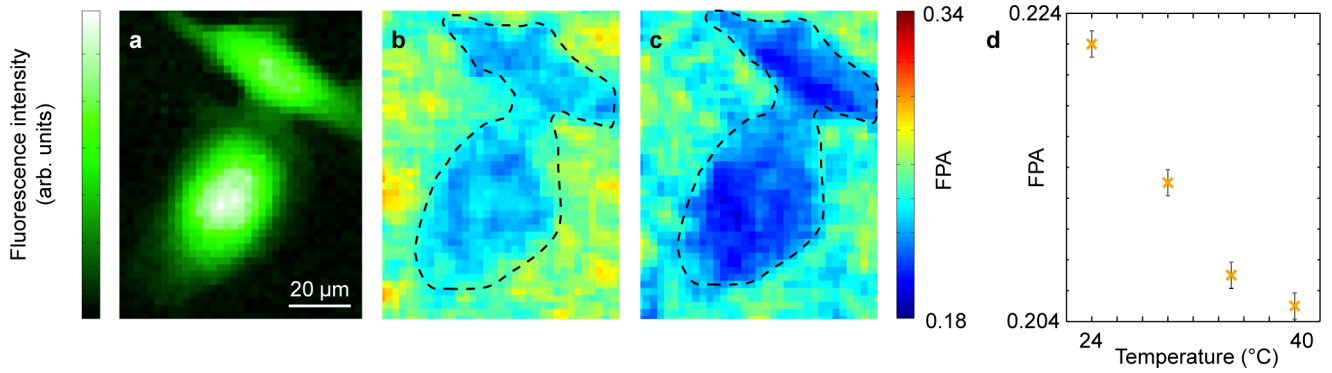

Figure 2. FPA measurements in HeLa cells while changing chamber temperature. (a) Intensity of fluorescence of GFP transfected HeLa cells excited with a blue laser. (b) FPA measured at T = 23 °C. (c) FPA at T = 40 °C. (d) Calibration curve that relates the measured FPA of the intracellular GFP with temperature.

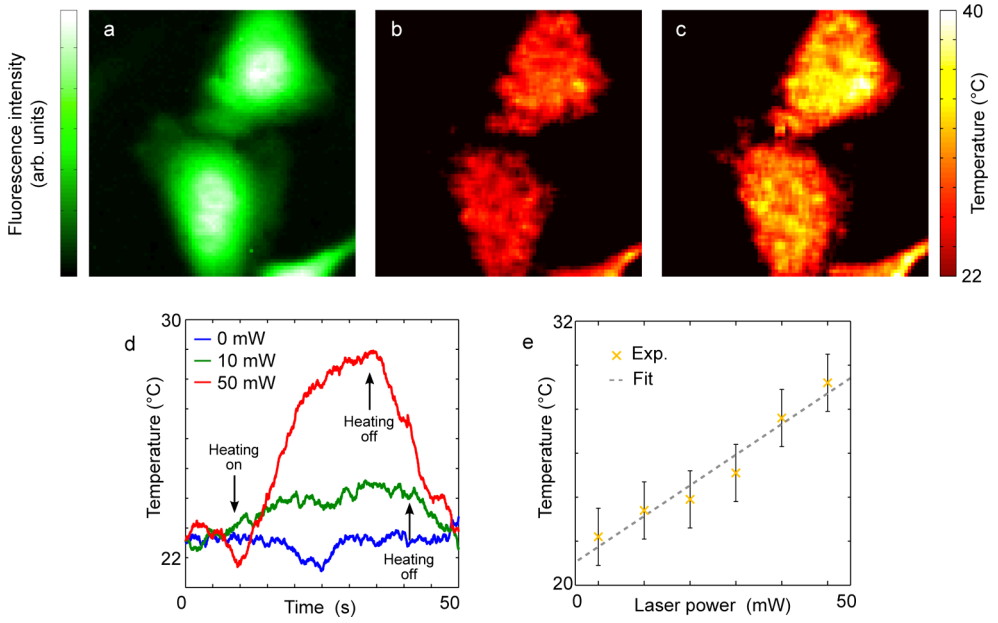

Figure 3. Temperature measurements in HeLa cells while delivering local heat via photothermal approach. (a) Fluorescence intensity of GFP transfected HeLa cells. (b) Temperature map while not heating. (c) Temperature map while heating the NR with a focused infrared laser with a power of P = 50 mW, located 50 μm to the right of center of the image. (d) Temperature variation of a point within the cell as function of time. (e) Temperature of a point within a cell for different laser heating powers.

cancer cells in which GFP was overexpressed as singular, nontagged proteins. Using transfected cells ensures that GFP occupies the entire cell volume. The temperature is processed from the FPA using the same procedure as in the case of GFP in PBS. However, the calibration curve relating temperature with FPA inside cells is different, since the intracellular viscosity differs from that of PBS. In order to obtain a new calibration curve, a resistive heating of the sample chamber was performed while recording the inner FPA of transfected HeLa cells as a function of the chamber temperature T_0. This calibration curve is presented in Figure 2d. FPA images for T_0 = 23 °C and T_0 = 40°C are shown in Figure 2 panels b and c, respectively. Interestingly, the FPA map inside the cell is uniform although the intensity map (Figure 2a) is not (due to a non-homogeneous distribution of GFP in the different organelles). This observation illustrates the fact that FPA is not dependent on fluorescence intensity, and that a probe the size of GFP experiences a uniform intracellular viscosity.[25] The uniform FPA map also suggests that the GFP did not interact with specific intracellular structures or cell components, which is an assumption that has been previously reposted.[26]

After obtaining the calibration curve associated with HeLa cells, we performed an experiment in which we heated by focusing an IR laser on gold nanorods (NR) dispersed in the extracellular medium. Using gold nanoparticles as nanosources of heat has many advantages compared to a universal resistive heating of the chamber. (i) It allows for local delivery of heat, which is fundamentally the best approach to investigate thermal biology at the single cell level; (ii) temperature variations can be fast and as brief as a few microseconds due to the weak thermal inertia of the small heated volume; and (iii) using gold NR matches the approach already considered in the fields of photothermal cancer therapy[27−29] or drug delivery.[30] We chose to locally heat the cells by focusing the IR laser 50 μm aside from the studied cell. In this work, we chose not to shine on the cell directly to demonstrate that FPA variations measured in the cytosol are unambiguously due to temperature variations and not to a possible IR-assisted perturbation of the GFP

dx.doi.org/10.1021/nl300389y | Nano Lett. 2012, 12, 2107−2111

fluorescence emission process. Temperature maps without and with heating are presented in Figure 3b,c, respectively. A temperature increase of around 8 °C is observed for a laser power of 50 mW focused over an area of about 1 μm in radius. For many applications, the temporal evolution during the cell metabolism is of pivotal interest. In Figure 3d, the temperature was measured in a fixed position and recorded as a function of time for different heating powers. The data was collected with a time resolution of 20 ms. The heating laser was focused 50 μm aside from the studied cell and abruptly turned on and off using a beam shutter. The temperature in the cell rises after the laser is turned on and falls as it is turned off with a characteristic time of 10 s. Thermalization times of few seconds are expected and have been previously reported[31] in systems where the heating volume is of mm^3 dimensions. Although we focus the heating laser to a 1 μm^2 spot, the illuminated volume above this focal point is also heated, due to the NR which are dispersed throughout the medium and act as heat sources, leading to a heating volume of a few mm^3. Furthermore, as expected, the temperature rises linearly with the intensity of the heating laser as observed in Figure 3e. A temperature error associated to this measurement was obtained by performing a standard deviation calculation of the collected data, giving 1.2 °C. Similar experiments were performed on U-87 MG cells and are presented in the Supporting Information section (Figure S2).

The presented method combines the advantages of high spatial resolution, good temperature accuracy with high biological compatibility, and fast readout. On the basis of these unique advantages, it has the potential to become a powerful tool to unravel intimate cellular processes that involve heating at the single cell level. Moreover, we foresee various natural extensions of the method that will further expand its capabilities. Higher temperature sensitivity can be achieved by engineering the properties of the fluorescent protein (modifying either fluorescence lifetime or hydrodynamic volume) resulting in τ_R closer to τ_F. Customization of the method for a specific system could be achieved by using a GFP derivative that absorbs light and fluoresces at a different spectral range. This method can be used in conjunction with the plethora of already developed techniques that use GFP fluorescence allowing two or more simultaneous measurements such as measuring temperature and pH at the same time.

■ ASSOCIATED CONTENT

Ⓢ Supporting Information

Figures S1–S3 and a description of materials and methods. This material is available free of charge via the Internet at http://pubs.acs.org.

■ AUTHOR INFORMATION

Corresponding Author

*E-mail: romain.quidant@icfo.es.

Author Contributions

‖These authors contributed equally to this work

Notes

The authors declare no competing financial interest.

■ ACKNOWLEDGMENTS

This work was supported by the European Commission's Seventh Framework Programme under Grants SPEDOC (248835), ERC-Plasmolight (259196), and Fundació Privada CELLEX. The authors also thank C. A. Ortega for technical help with cell transfection; E. Bermudez for the fabrication of the gold nanostructures; and Dr. S. Balint and Dr. A. Adams for critical discussions.

■ REFERENCES

(1) Kamei, Y.; Suzuki, M.; Watanabe, K.; Fujimori, K.; Kawasaki, T.; Deguchi, T.; Yoneda, Y.; Todo, T.; Takagi, S.; Funatsu, T.; Yuba, S. *Nat. Methods* **2009**, *6*, 79–81.

(2) Lowell, B. B.; Spiegelman, B. M. *Nature* **2000**, *404*, 652–660.

(3) Andrews, Z. B.; Diano, S.; Horvath, T. L. *Nat. Rev. Neurosci.* **2005**, *6*, 829–840.

(4) Yang, J. -M.; Yang, H.; Lin, L. *ACS Nano* **2011**, *5*, 5067–5071.

(5) Maestro, L. M.; Rodríguez, E. M.; Rodríguez, F. S.; Iglesias-de la Cruz, M. C.; Juarranz, A.; Naccache, R.; Vetrone, F.; Jaque, D.; Capobianco, J. A.; Solé, J. G. *Nano Lett.* **2010**, *10*, 5109–5115.

(6) Gota, C.; Okabe, K.; Funatsu, T.; Harada, Y.; Uchiyama, S. *J. Am. Chem. Soc.* **2009**, *131*, 2766–2767.

(7) Vetrone, F.; Naccache, R.; Zamarrón, A.; Juarranz de la Fuente, A.; Sanz-Rodríguez, F.; Martinez Maestro, L.; Martín Rodriguez, E.; Jaque, D.; Solé, J. G.; Capobianco, J. A. A. *ACS Nano* **2010**, *4*, 3254–3258.

(8) Zohar, O.; Ikeda, M.; Shinagawa, H.; Inoue, H.; Nakamura, H.; Elbaum, D.; Alkon, D. L.; Yoshioka, T. *Biophys. J.* **1998**, *74*, 82–89.

(9) McCabe, K. M.; Lacherndo, E. J.; Albino-Flores, I.; Sheehan, E.; Hernandez, M. *Appl. Environ. Microbiol.* **2011**, *77* (9), 2863–2868.

(10) Wang, C.; Xu, R.; Tian, W.; Jiang, X.; Cui, Z.; Wang, M.; Sun, H.; Fang, K.; Gu, N. *Cell Res.* **2011**, *21*, 1517–1519.

(11) Zimmer, M. *Chem. Soc. Rev.* **2009**, *38*, 2823–2832.

(12) Day, R. N.; Davidson, M. W. *Chem. Soc. Rev.* **2009**, *38*, 2887–2921.

(13) Frommer, W. B.; Davidson, M. W.; Campbell, R. E. *Chem. Soc. Rev.* **2009**, *38*, 2833–2841.

(14) Tsien, Y. *Annu. Rev. Biochem.* **1998**, *67*, 509–544.

(15) Zimmer, M. *Chem. Rev.* **2002**, *102*, 759–782.

(16) Llopis, J.; McCaffery, J. M.; Miyawaki, A.; Farquhar, M. G.; Tsien, R. Y. *Proc. Natl. Acad. Sci. U.S.A.* **1998**, *95*, 6803–6808.

(17) Valeur, B. *Molecular Fluorescence: Principles and Applications*; Wiley: New York, 2007.

(18) Baffou, G.; Kreuzer, M. P.; Kulzer, F.; Quidant, R. *Opt. Express* **2009**, *17*, 3291–3298.

(19) Baffou, G.; Girard, C.; Quidant, R. *Phys. Rev. Lett.* **2010**, *104*, 136805.

(20) Zondervan, R.; Kulzer, F.; Van der Meer, H.; Disselhorst, J. A. J. M.; Orrit, M. *Biophys. J.* **2006**, *90*, 2958–2969.

(21) Sample, V.; Newman, R.; Zhang, J. *Chem. Soc. Rev.* **2009**, *38*, 2852–2864.

(22) Bockman, S. H.; Ward, W. W. *Biochem. Biophys. Res. Commun.* **1981**, *101*, 1372–1380.

(23) Hink, M. A.; Griep, R. A.; Borst, J. W.; van Hoek, A.; Eppink, M. H. M.; Schots, A.; Visser, A. J. W. G. *J. Biol. Chem.* **2000**, *275*, 17556–17560.

(24) Busch, N. A.; Kim, T.; Bloomfield, V. A. *Macromolecules* **2000**, *33*, 5932–5937.

(25) Kalwarczyk, T.; Ziebacz, N.; Bielejewska, A.; Zaboklicka, E.; Koynov, K.; Szymanski, J.; Wilk, A.; Patkowski, A.; Gapinski, J.; Butt, H. J.; Holyst, R. *Nano Lett.* **2011**, *11*, 2157–2163.

(26) Swaminathan, R.; Hoang, C. P.; Verkman, A. S. *Biophys. J.* **1997**, *72*, 1900–1907.

(27) Hirsch, L. R.; Stafford, R. J.; Bankson, J. A.; Sershen, S. R.; Rivera, B.; Price, R. E.; Hazle, J. D.; Halas, N. J.; West, J. L. *Proc. Natl Acad. Sci. U.S.A.* **2003**, *100* (23), 13549–13554.

(28) Lal, S.; Clare, S. E.; Halas, N. J. *Acc. Chem. Res.* **2008**, *41*, 1842–1851.

(29) Bardhan, R.; Lal, S.; Joshi, A.; Halas, N. J. *Acc. Chem. Res.* **2011**, *44*, 936–946.

(30) Luo, Y.-L.; Shiao, Y.-S.; Huang, Y. -F. *ACS Nano* **2011**, *5* (10), 7796–7804.

(31) Richardson, H. H.; Carlson, M. T.; Tandler, P. J.; Hernandez, P.; Govorov, A. O. *Nano Lett.* **2009**, *9*, 1139−1146.

dx.doi.org/10.1021/nl300389y | *Nano Lett.* 2012, 12, 2107−2111